Journal of Chromatography B, 878 (2010) 1973–1981

Contents lists available at ScienceDirect

Journal of Chromatography B

journal homepage: www.elsevier.com/locate/chromb

Characterization of a unique IgG1 mAb CEX profile by limited Lys-C proteolysis/CEX separation coupled with mass spectrometry and structural analysis

Jaewon Kim[a,*,1], Laurie Jones[a,1], Lisa Taylor[a,1], Gunasekaran Kannan[b], Frank Jackson[c], Hollis Lau[a], Ramil F. Latypov[a], Bob Bailey[a,*]

[a] Department of Analytical & Formulation Sciences, 1201 Amgen Court West, Seattle, WA 98119-3105, USA
[b] Protein Sciences, 1201 Amgen Court West, Seattle, WA 98119-3105, USA
[c] Cellular Resources, Amgen Inc. 1201 Amgen Court West, Seattle, WA 98119-3105, USA

ARTICLE INFO

Article history:
Received 9 December 2009
Accepted 20 May 2010
Available online 1 June 2010

Keywords:
Monoclonal antibody
Cation exchange chromatography
Limited Lys-C proteolysis
Mass spectrometry
Structural analysis

ABSTRACT

The unique cation exchange chromatography (CEX) charge variant profile of mAb1 is characterized by a combination of mass spectrometry, limited Lys-C digestion followed by CEX separation and structural analysis. During CEX method development, mAb1 showed several unexpected phenomena, including a unique profile containing two main species (acidic 2 and main) and significant instability during stability studies of the main species. Reduced Lys-C peptide mapping identified a small difference in one of the heavy chain peptides (H4) in acidic 2 and further mass analysis identified this difference as Asn55 deamidation. However, the amount of Asn55 deamidation in acidic 2 could account for only half of the species present in this peak. Lys-C limited digest followed by CEX separated several unique peaks in the acidic peak 2 including two pre Fab peaks (LCC1 and LCC2). Whole protein mass analysis suggested that both LCC1 and LCC2 were potentially deamidated species. Subsequent peptide mapping with MS/MS determined that LCC1 contained isoAsp55 and LCC2 contained Asp55. Combining LCC1 and LCC2 CEX peak areas could account for nearly all of the species present in acidic peak 2. Subsequent detailed sequence analysis combined with molecular modeling identified Asn55 and its surrounding residues are responsible for the different CEX behavior and instability of mAb1 following forced degradation at high pH. Overall, the combinatorial approach used in this study proved to be a powerful tool to understand the unique charge variant and stability profile of a monoclonal antibody.

1. Introduction

Therapeutic monoclonal antibodies (mAbs) have developed rapidly into a very beneficial and profitable market, most in the treatment of cancer and autoimmune diseases. At least 18 monoclonal antibodies have been developed for various therapeutic purposes and many more are undergoing clinical trials [1,2]. Even though mAbs are generally stable molecules, various chemical and/or physical modifications during the expression, product purification and storage create product related heterogeneity. Approval of therapeutic mAbs by regulating agencies requires development of robust and reproducible analytical methods that can identify and characterize minor impurities and heterogeneities. ion exchange chromatography (IEX) HPLC is a routine and popular analytical method to assess the charge related heterogeneity of mAbs. Several factors can contribute to charge heterogeneity, including structural isoforms, glycosylation, glycation, oxidation, deamidation, isomerization and peptide cleavage [3,4]. The complexity of charge variants often imposes formidable challenges to assess the complete charge variant profile.

Several approaches have been developed to simplify the intact mAbs charge variant characterization. One way is to utilize the fact that the mAb hinge area is more exposed than other areas, which allows for the use of limited proteolysis to separate the Fab and Fc domains for further analysis. Papain has been the most commonly used protease to cleave IgG1 into bivalent or univalent Fab and Fc peptides [5–7]. However, the down side for papain digest is that it has a broad specificity for digestion and the necessity of cysteine for the reaction, which could generate undesirable cysteinylation [8]. Lys-C became a popular alternative protease, due to its high specificity and less procedure related artifacts [9,10]. Another way to simplify the IEX profile is to reduce mAbs, which

* Corresponding authors.
E-mail addresses: jaewonk@amgen.com (J. Kim), baileyrw@amgen.com (B. Bailey).
[1] Equal contribution.

1570-0232/$ – see front matter © 2010 Elsevier B.V. All rights reserved.
doi:10.1016/j.jchromb.2010.05.032

generates light chain (LC) and heavy chain (HC) [11]. After the mAbs are fragmented, either by limited proteolysis and/or reduction, the mAb components can be separated by cation exchange chromatography (CEX) [12] or RP-HPLC [13–16] for further identification and characterization.

Recently, we have developed Lys-C limited proteolysis coupled with a CEX separation method (Lys-C/CEX), which was proven very powerful for the characterization of several mAbs [17]. Lys-C/CEX has several advantages compared to other methods such as eliminating artifacts from the harsh running conditions of RP-HPLC and easy fractionation for further characterization.

Deamidation of asparagine (Asn) residues is a common chemical modification of mAbs. Without proper formulation or storage conditions, non-enzymatic deamidation could be a major cause of mAb degradation. Moreover, the deamidation event can have serious implications for drug efficacy in mAbs and other therapeutic proteins [15,18,19]. Asn deamidation occurs through the formation of a cyclic imide (succinimide) intermediate followed by spontaneous hydrolysis into a mixture of isoaspartic acid (isoAsp) or aspartic acid (Asp) [20,21]. It is known that isoAsp formation is favored over the formation of Asp (3:1 ratio), however this may be influenced by the secondary and tertiary structure [22,23]. Deamidation rates had been assessed using pentapeptides, and it was identified that glycine flanking a C terminal Asn exhibited the fastest deamidation rate [20,24]. Furthermore, based on the available protein tertiary structure, structure-dependent deamidation rates were calculated [25]. It was suggested that in proteins, Asn deamidation rate depends 60% on primary sequence and 40% on three-dimensional structure [25,26]. For mAbs, several groups have identified possible Asn deamidation sites and their rate within constant and variable regions by using HPLC–MS analysis [15,27].

In this study, we utilized peptide mapping, Lys-C limited proteolysis and primary/tertiary structure analysis to elucidate a unique mAb CEX profile.

2. Experimental

2.1. Chemicals and reagents

The mAbs used for the study were expressed in Chinese hamster ovary cells (CHO) and manufactured at Amgen and purified using standard procedures [28].

2.2. Cation exchange chromatography and fractionation

The mAbs were run on a Dionex Propac® WCX-10 column (4.0 mm × 250 mm) using an Agilent 1200 HPLC and were monitored at 214 and 280 nm. The solvents were (A) 20 mM sodium acetate and (B) 20 mM sodium acetate, 500 mM NaCl, pH 5.6. The column was equilibrated with 95% A, the gradient generated was 5–50% B over 30 min with a flow rate of 0.8 mL/min. The final CEX method performance was tested with regard to specificity, load linearity, precision (repeatability and intermediate precision), accuracy and quantification limit. For the fractionation, we used a preparative column (Dionex Propac® WCX-10, 22 mm × 250 mm) followed by a semi-prep column (Dionex Propac® WCX-10, 9 mm × 250 mm) with the same running buffer and conditions.

2.3. Reduced and alkylated Lys-C and Asp-N peptide map

The mAbs and purified fragments were reduced with 10 mM dithiothreitol (DTT) and alkylated with 22 mM iodoacetic acid (IAA) at pH 8.3. The reduced and alkylated molecule was then digested with Promega endoproteinase Lys-C enzyme (10 min, 37 °C) and with Asp-N (4 h, 37 °C) with an enzyme to substrate ratio of 1:10. Peptides resulting from the Lys-C/Asp-N digestion were separated by reversed-phase chromatography on an Agilent Zorbax SB-C3 chromatography column at a flow rate of 0.2 mL/min. The reversed-phase chromatography solvents were (A) 0.12% triflouroacetic acid (TFA) (w/v) and (B) 0.11% TFA (w/v) in 80% acetonitrile. Eluted peaks were detected at 214 nm. LC–MS identification of the peptides was performed on an Agilent 1100 series HPLC coupled to an Agilent LC/MSD SL iontrap mass spectrometer. Prior to use the mass spectrometer was calibrated with the manufactured supplied calibration standard and calibration procedure. Bruker Daltonics Data Analysis software was utilized for the analysis of MS and MS/MS data.

2.4. Whole protein mass analysis

The mAbs were diluted to 1 mg/mL in water prior to a 5 μg injection onto a polyhydroxyethyl A chromatography column (Poly LC) to remove residual salts from the sample. An isocratic gradient of 0.1% formic acid in water at 0.1 mL/min was utilized with the addition of a post column tee of 98% acetonitrile and 2% formic acid flowing prior to the in-line Agilent 6210 TOF mass spectrometer. Mass spectrometry parameters included a capillary voltage setting of 5000 V. Prior to use the mass spectrometer was calibrated with the manufactured supplied calibration standard and calibration procedure. Agilent Mass Hunter software was used to deconvolute and analyze the mass spectral data.

2.5. Non-reducing tryptic peptide map

The mAbs were partially denatured in 2 M Urea, 0.1 M Tris, pH 8 and 10% acetonitrile and digested overnight with Roche trypsin (enzyme:substrate ratio of 1:10) at 37 °C. The resulting peptides were evaluated on a Jupiter C4 (Phenomenex) chromatography column with an acetonitrile and triflouroacetic acid gradient run on an Agilent 1100 series HPLC with an in-line Agilent LC/MSD SL iontrap mass spectrometer. Bruker Daltonics Data Analysis software was utilized for the analysis of MS and MS/MS data.

2.6. Limited Lys-C digestion and peptide fractionation

A 500 μL volume of mAb1 at a concentration of 50 mg/mL was combined with 125 μg of endoproteinase Lys-C for a final enzyme:substrate ratio of 1:200. Sample was incubated at 37 °C for 5 min at which point the digestion was quenched by the addition of 125 μL of 150 mM ammonium acetate at pH 4.7. CEX was performed at ambient temperature on a Dionex ProPac® WCX-10 analytical column (4 mm × 250 mm) proceeded by a Dionex Propac WCX-10 guard column. The solvents were (A) 20 mM sodium acetate, pH 5.2, (B) 20 mM sodium acetate, 300 mM sodium chloride, pH 5.2. The column was equilibrated with 95% (A) and the gradient was generated from 5% to 100% (B) over 35 min. A 10 μL (400 μg after quenching) sample was injected onto the column and analyzed at a flow rate of 0.7 mL/min.

2.7. Structure analysis

The Fab regions of mAb1 and mAb2 were modeled based on a homology modeling procedure adapted from Molecular Operating Environment software (MOE, *Chemical Computing Group, Inc.*). For each antibody, 25 structures were generated using the MOE software and the final structure corresponded closest to the mean structure as identified by the α-Carbon Root Mean Square Deviation (C^{α} RMSD). The final structure was then refined using CHARMM22 forcefield. The quality of the refined final structures in both cases appeared to be reasonable as only a few residues adopted disallowed conformations in the Ramachandran Map.

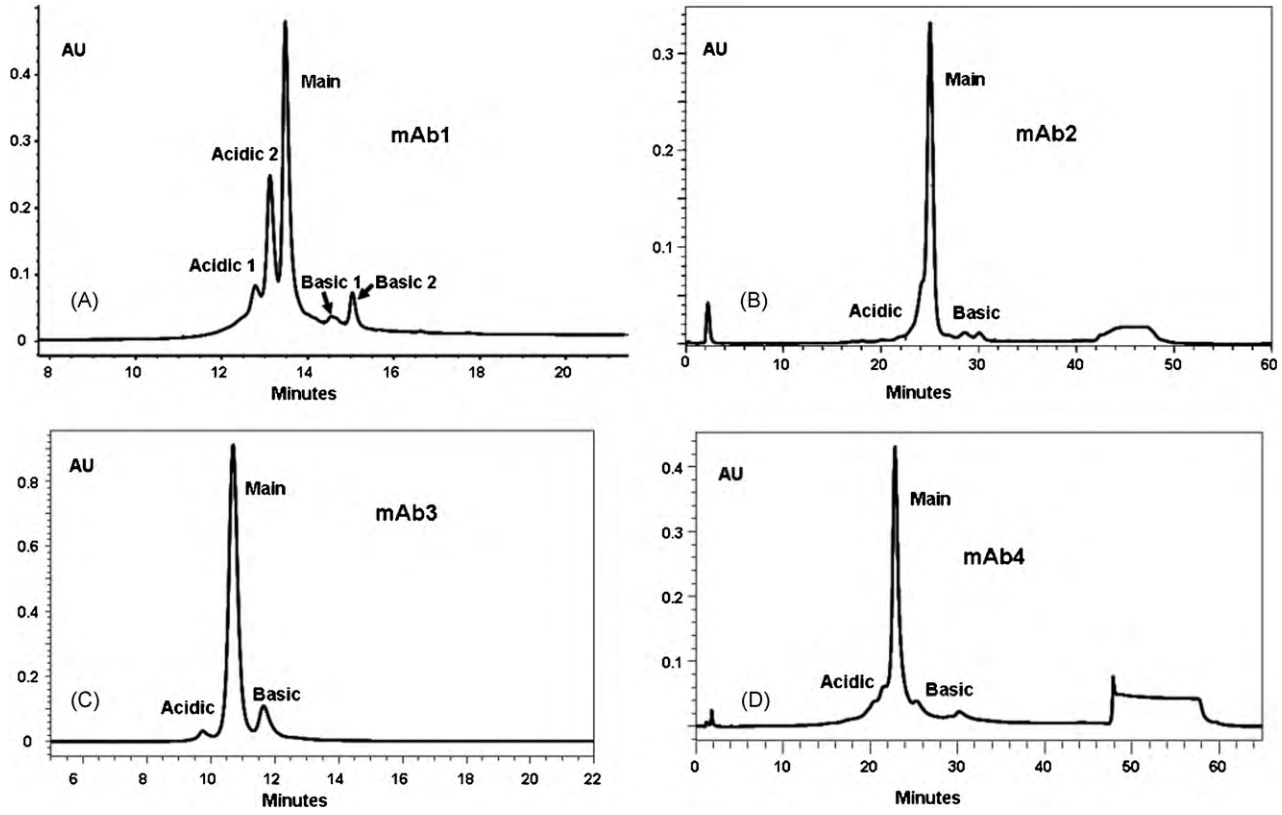

Fig. 1. Cation exchange chromatography (CEX) profiles of 4 IgG1 mAbs (A–D). mAb1 displayed a significantly different CEX profile with a large amount of acidic variants.

3. Results and discussion

3.1. Unique mAb1 CEX profile

The mAb1 theoretical isoelectric point (p*I*) was confirmed by capillary isoelectric focusing (cIEF) and used to select the initial CEX buffer. After the optimization process, including different mobile phase pH values, salt concentration and buffer gradients, the final CEX method displayed well resolved charge variants of mAb1 (Fig. 1A). We assigned the largest peak as main (13.5 min elution) and earlier eluted peaks as acidic peak 1 (12.8 min) and acidic peak 2 (13.2 min) and later eluted peaks as basic 1 (14.7 min) and 2 (15.1 min). The mAb1 CEX profile showed a very large amount of acidic species (~40%) including notably a large acidic peak 2 species. Comparison of the mAb1 CEX profile with three other IgG1 CEX profiles clearly showed that the mAb1 CEX profile was unique (Fig. 1B–D). Since the mAb1 was an aglycosylated molecule, it was of great interest to understand the unusual CEX profile. Previously, several IgG1 CEX profiles showed high heterogeneity related to sialylation [29]. Since mAb1 is aglycosylated, sialylation is not an explanation for the high amount of acidic species. In addition to sialylation, unprocessed lysine contributes to the CEX basic charge heterogeneity [29–31]. The C-terminus lysine residue of mAbs is typically hydrolyzed during secretion into culture media. The effect of lysine on CEX charge heterogeneity can be investigated using carboxypeptidase B, which hydrolyzes basic residues at the C-terminus. Carboxypeptidase B treated mAb1 displayed a similar CEX profile indicating the unique mAb1 CEX profile was not from unprocessed C-terminus lysine.

3.2. Forced degradation study

To further investigate the nature of the unique CEX charge profile, forced degradation studies (extreme pH, elevated temperature and forced oxidation) were performed on mAb1 and analyzed by CEX. MAb1 was dialyzed into pH 8.0 buffer and incubated at 40 °C and analyzed at different time points (3 days, 1, 2 and 4 weeks) (Fig. 2A). The CEX profile of the degraded mAb1 samples showed that mAb1 was extremely labile. The main peak species rapidly converted to the acidic region after 3 days of incubation (Fig. 2A, blue trace). To compare the degree of degradation of other mAbs to mAb1, we performed forced degradation on two other IgG1 s (Fig. 2B). The results showed that mAb1 was the most labile (lost ~40% main species after 3 days), whereas the other two IgGs did not change in the same time period. To determine whether the lack of glycosylation was the reason for the unusual CEX profile and decreased stability of mAb1, we evaluated the CEX and stability profile of glycosylated mAb1. Glycosylated mAb1 exhibited a similar CEX profile to the aglycosylated form although the acidic peak 1 and 2 species were slightly higher (Fig. 3A and C). Glycosylated mAb1 also displayed a similar stability profile to aglycosylated mAb1, indicating glycosylation was not the reason for the unique mAb1 CEX and stability profiles (Fig. 3B and D).

3.3. Charge variants fractionation and Lys-C peptide mapping

To further characterize the physical/chemical attributes of the mAb1 charge variants, we enriched each charge variant (>90% purity) using preparative CEX separation followed by semi-preparative CEX separation (data not shown). Using the highly enriched fractions, we assessed their physical stability by using several techniques such as differential scanning calorimetry (DSC), circular dichroism (CD), and non-reducing peptide mapping analysis. The results eliminated any physical or conformational differences among the CEX charge variants (data not shown). We performed reduced Lys-C peptide mapping of mAb1 to identify chemical modifications in the charge variants. Reduced Lys-C digestion resulted in a less complex chromatographic profile with fewer

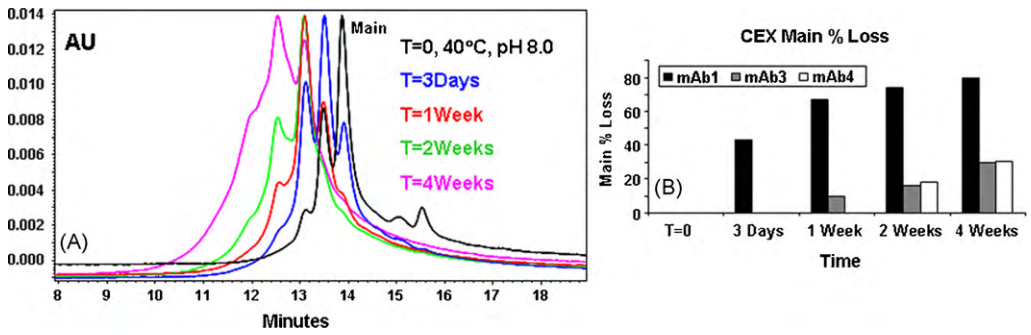

Fig. 2. (A) The forced degradation mAb1 CEX profile at pH 8.0, 40 °C (B) Main species percent loss comparison for all the IgG1 mAbs. MAb1 CEX main species lost more than 50% to acidic species after just 3 days, which is extremely labile compared to two other IgG1 mAbs at the same conditions (both lost ~30% main species after 4 weeks incubation.

co-eluting peptides (total of 31 HC and 12 LC peptides) than a tryptic digestion. Comparison of the reduced Lys-C peptide maps of the main and acidic peak 2 species of mAb1 displayed several minor differences. The H4 Lys-C peptide showed the most noticeable difference (Fig. 4A). The H4 peptide has 40 residues with a theoretical mass of 4502.9 Da. RP-HPLC separated H4 into two peaks (50.7 and 51 min), which were analyzed by tandem mass spectrometry. The tandem MS/MS of the 51 min peak displayed a mass increase on the *m*/*z* 1027.6 (y9), 1084.6 (y10) and 1171.6 (y11) ions indicating that a 1 Da increase was present due to the deamidation of Asn55 of mAb1 (Fig. 4C and D). However, the amount of deamidated Asn55 (51 min elution) calculated from Fig. 4A was only 18%, which could account for a maximum of 36% of the acidic peak 2, assuming the modification in an intact antibody.

3.4. Limited Lys-C proteolysis

Limited proteolysis using papain or Lys-C generates Fc and Fab antibody fragments that can result in simplified peptide mapping and analyses. We applied the Lys-C limited proteolysis coupled with CEX separation for mAb1 charge variants characterization. We optimized Lys-C limited proteolysis conditions and CEX separation for mAb1 to achieve the best separation of mAb1 Fab and Fc peptides (Fig. 5A). Lys-C/CEX separation of mAb1 displayed several peaks in addition to the peaks corresponding to Fab and Fc (Fig. 5A). To eliminate possible non-specific cleavage outside of the hinge lysine, we screened different Lys-C digestion conditions and the MS/MS confirmed that the unknown peaks were not from non-specific digestion (data not shown). The two peaks, eluting before the Fab peak, at 11.8 and 12 min were named LCC1 (Lys-C–CEX 1) and LCC2, respectively. LCC1 and LCC2 were noticeably large (~45%) in the acidic peak 2 and were almost absent in the main species (Fig. 5B). One of the minor post Fab peaks (16.3 min elution, Fig. 5B inset) was also different in the acidic peak 2 and was identified as Fab containing N-terminal glutamine (less than 8% of mAb1 contains N-terminal glutamine with the majority of mAb1 containing N-terminal pyroglutamic acid). The majority of the N-terminal glutamine containing Fab was detected in the basic fractions from the original CEX separation (data not shown). LCC1, LCC2 and the Fab peaks from Lys-C/CEX were purified for further analysis.

Whole protein mass analysis of protein fractions LCC1 and LCC2 using an Agilent LC-TOF displayed an approximate 1 Da mass increase for LCC1 and LCC2, 47478.35 (mass error 23.2 ppm) and 47478.65 (mass error 27.4 ppm), respectively, compared to the

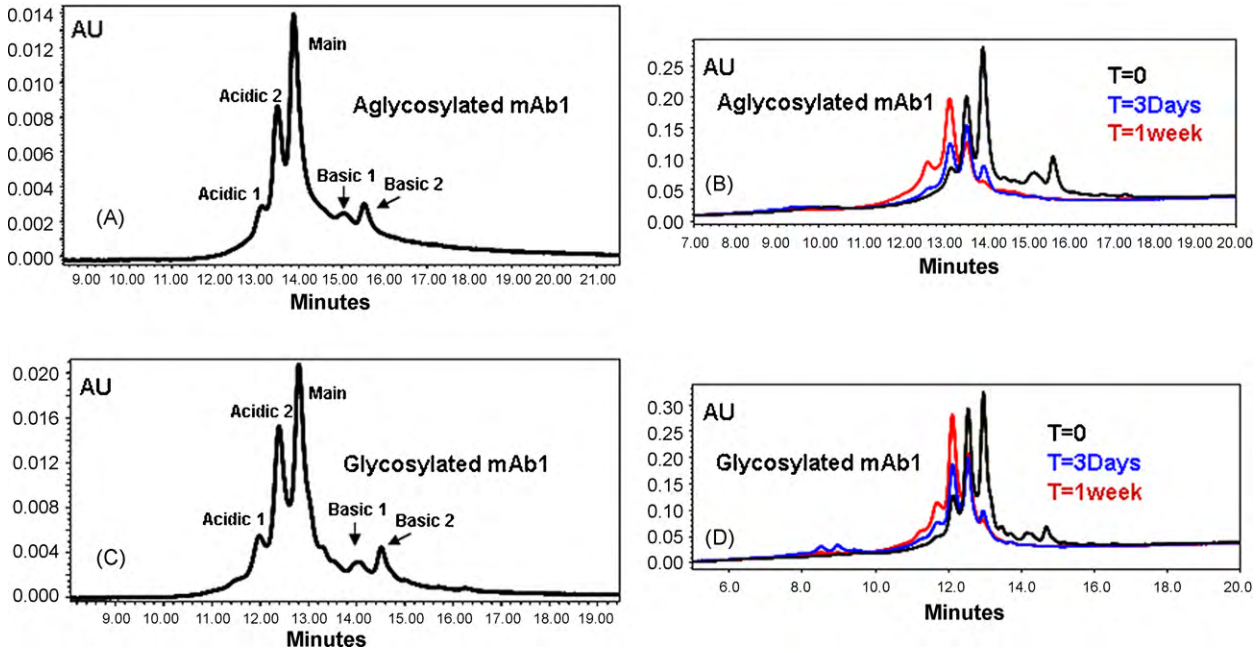

Fig. 3. CEX profile comparisons between aglycosylated and glycosylated mAb1 (A and C) and forced degradation profile between two others (B and D). Glycosylated mAb1 displayed a similar CEX profile with a slight increase in acidic species. Furthermore, glycosylated mAb1 showed a similar stability profile under stressed conditions compared to aglycosylated mAb1.

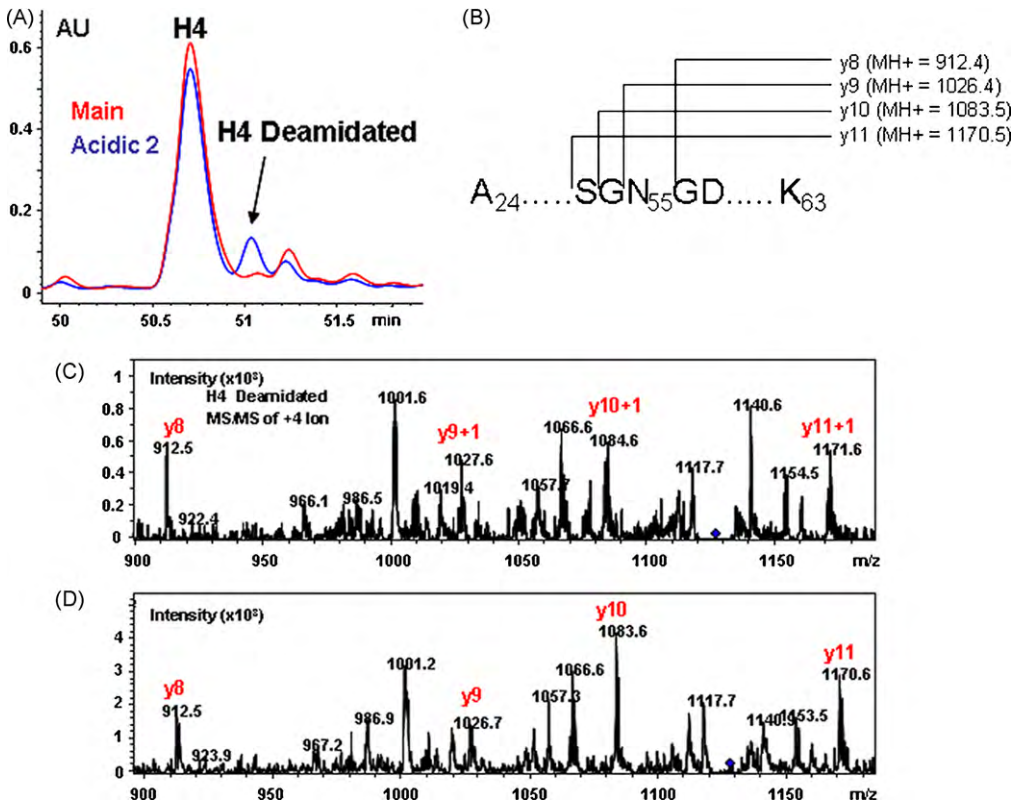

Fig. 4. Comparison of the reduced Lys-C peptide maps of highly enriched mAb1 main and acidic peak 2 (A) Overlay of the A214 UV traces of the mAb1 main and acidic peak 2 H4 peptides. (B) Expected MS/MS fragments and masses of the H4 peptide. (C) +4 MS/MS of the deamidated H4 peptide. (D) +4 MS/MS of unmodified H4 peptide. Unlabelled peaks within the MS/MS spectra correspond to other H4 fragment ions.

unmodified Fab mass of 47477.42 (mass error 2.1 ppm) (Fig. 6A–C). This difference in mass with higher mass error of LCC1 and LCC2 suggested that LCC1 and LCC2 could contain a deamidation or possibly a deamidation and an isomerization in one species and not the other, to account for differences in retention time between LCC1 and LCC2 in the CEX separation. However, given the precision of the instrument, deamidation or deamidation and isomerization was only speculative and could not be confirmed without further analysis with peptide mapping and MS/MS. In addition, there was an unknown species with a deconvoluted mass of 47,438 Da present only in the LCC1 collected peak along with a descending shoulder on the main species, indicating that other Fab modifications are present in the LCC1 fraction. These other species have not been identified.

The LCC1, LCC2 and Fab peaks collected from the Limited Lys-C/CEX method were further analyzed by non-reducing tryptic peptide mapping. A non-reducing peptide mapping approach was utilized to determine if any differences in the arrangement of disulfide bonds existed between LCC1 and LCC2 that could account for their differing retention times by CEX. This method also allowed us to determine if there was indeed a deamidation or deamidation and isomerization event on LCC1 and/or LCC2 that could account for the 1 Da mass shift observed by whole protein mass analysis. As previously mentioned, the non-reduced peptide map confirmed that the disulfide bonds were equivalent between LCC1, LCC2 and the Fab peak and ruled out a possible structural difference among LCC1 and LCC2 relating to disulfides (data not shown). This method did reveal a significant difference in the retention time of a single heavy chain peptide between LCC1, LCC2 and Fab. This peptide eluted at approximately 77.5 min in both LCC1 and Fab samples and at a later retention time of 79.1 min in LCC2 (Fig. 7A). Tandem MS/MS indicated that this peptide contained a 1 Da increase on heavy chain residue 55 in both LCC1 and LCC2 and the expected mass was observed in the Fab (Fig. 7B–D). This result suggests deamidation of Asn55 on both LCC1 and LCC2. It is known that isoAsp containing peptides elute earlier on peptide maps, where Asp containing peptides elute later than unmodified peptides [18,32–34]. Therefore, it is plausible that the LCC1 fraction consists of Fab with a deamida-

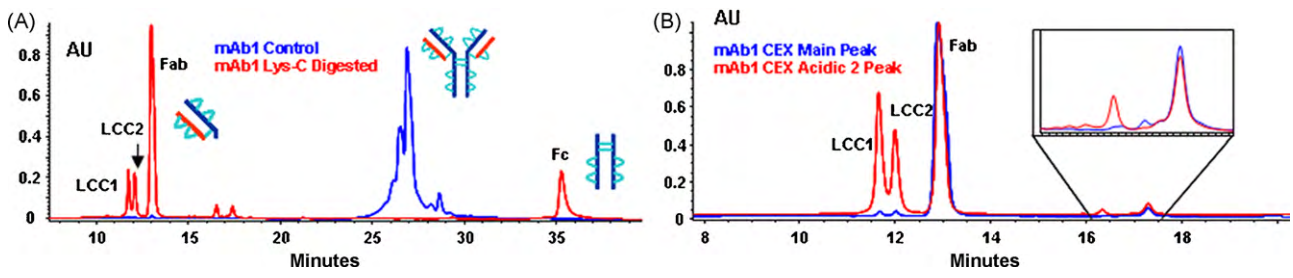

Fig. 5. MAb1 Lys-C limited proteolysis coupled with CEX separation. (A) CEX separation comparison between control and Lys-C digested mAb1 (B) Lys-C digestion coupled with CEX separation comparison between main and acidic peak 2 species.

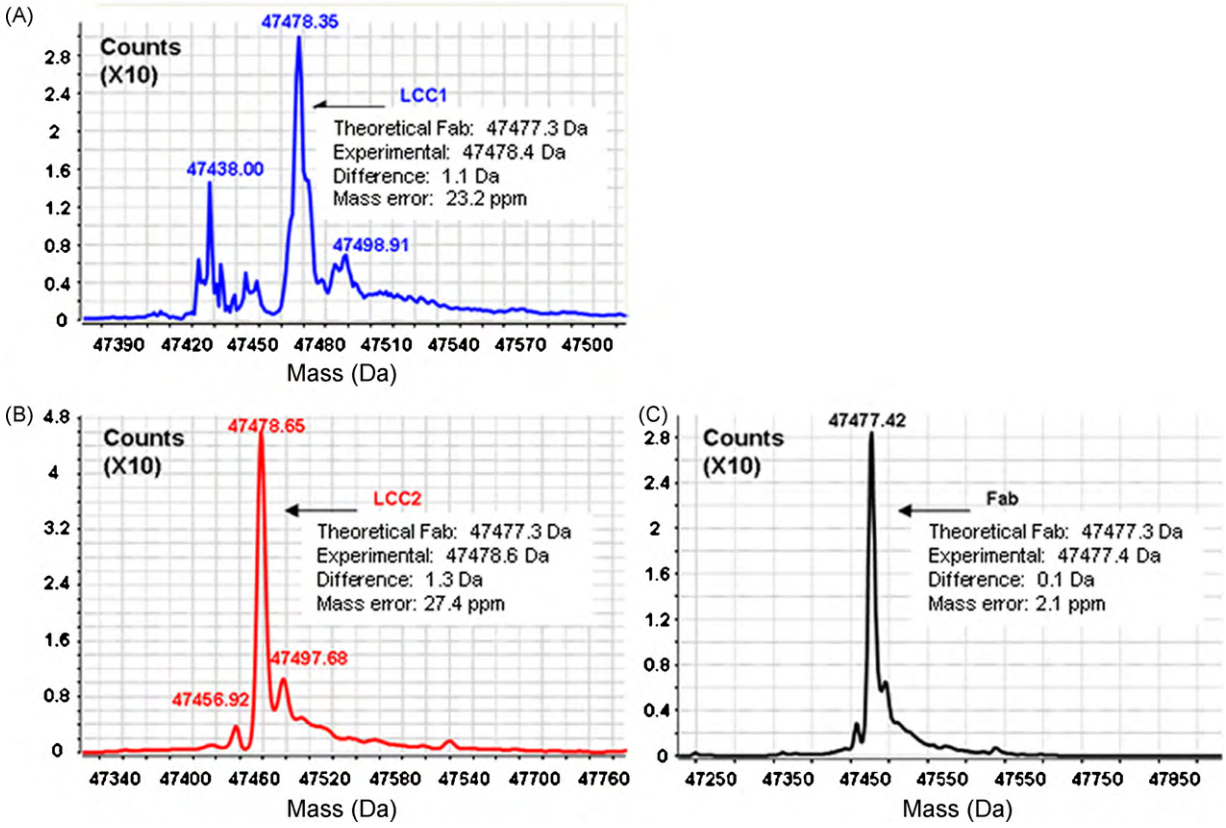

Fig. 6. Whole protein mass analysis of highly enriched LCC1, LCC2 and Fab (A–C) after Lys-C digest/CEX separation of mAb1.

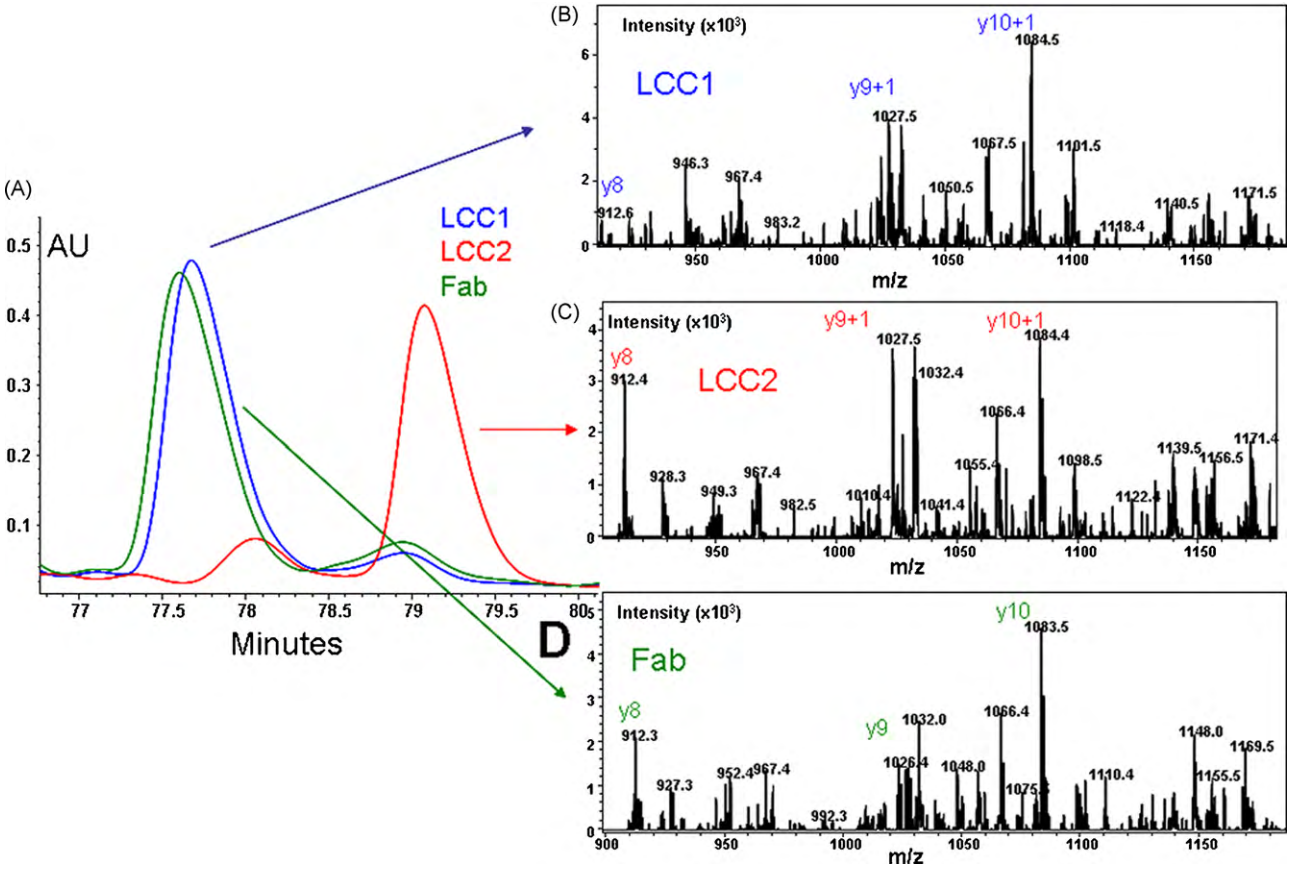

Fig. 7. Non-reducing tryptic peptide map of Lys-C/CEX Fab collected fractions. (A) Overlay of the A214 UV chromatogram (B–D) MS/MS of the +3 ion of the tryptic peptide containing heavy chain residue 55.

Table 1
Percentage of LCC1, LCC2 and Fab from mAb1 CEX fractions.

mAb1 CEX fractions	% LCC1 (D_{55})	% LCC2 ($^{iso}D_{55}$)	% Fab	% D_{55} + $^{iso}D_{55}$	
				Reduced mAb	Predicted range in intact mAb
CEX acidic 1	31.99	23.56	44.45	55.5	55–100
CEX acidic 2	27.39	19.16	53.44	46.6	46.6–93.2
CEX main	1.18	1.27	97.55	2.5	2.5–5

tion and isomerization at residue 55. The later retention time of the residue 55 containing peptide in the LCC2 fraction in the peptide map is explained by the deamidation of residue 55. Combining peak areas of LCC1 and LCC2 from acidic peak 2 and dividing by the total Fab area (LCC1 + LCC2 + Fab peak areas) results in ~47%. This modification therefore could account for approximately 94% of intact molecules in the acidic 2 peak. Combining LCC1 and LCC2 could also account for the majority of the species present in acidic peak 1 in an intact antibody (Table 1). Additional deamidation/isomerization identified on an asparagines residue in the Fc region of the antibody could explain the different elution of the acidic peak 1 species (data not shown).

The original reduced and alkylated peptide mapping analysis of the acidic peak 2 compared to the main CEX peak (Fig. 4) was not capable of separating the deamidated and isomerized peptide from the unmodified peptide due to the co-elution of these species. Given the precision of the iontrap mass spectrometer and the only 1 Da mass difference in these co-eluting species made the identification of the modified species impossible by that method. By separating the deamidated and isomerized Fab from the unmodified Fab with the limited Lys-C/CEX method and performing subsequent peptide mapping on these species (Fig. 7), it was possible to identify this additional deamidated and isomerized form of residue 55 and account for the majority of the species present in the acidic 2 peak.

3.5. Selective digestion by Asp-N

We have identified that LCC1 and LCC2 contain isoAsp and Asp at residue 55, respectively, by using whole mass, reduced and native peptide map analysis. To confirm the identity of LCC1 and LCC2, we utilized an additional endoprotease, Asp-N. It is known that Asp-N cannot cleave peptide bonds N-terminal to isoAsp [35]. Therefore, it was hypothesized that LCC1 and LCC2 should generate different fragments by Asp-N, if they contain isoAsp and Asp, where the native peptide contains Asn in the same position. Indeed, LCC1, LCC2 and unmodified Fab showed a different fragment pattern between 48 and 51 min by RP-HPLC (Fig. 8A and B). Mass analysis of each unique fragment identified the specific digestion site in the Asp-N H2 peptide (Fig. 8 C and D). The unmodified Fab fraction from the limited Lys-C digestion was cut by Asp-N before D_{57} as expected. Unlike unmodified Fab, the LCC2 fraction of Lys-C digestion was cut before the deamidated residue D55, which confirmed the previous conclusion (Fig. 8C). LCC1, which is identified as isoAsp at the residue 55 was not cut by Asp-N at the 55 or 57 position. It is known that iso-Asp causes the miscleavage of neighboring residues [36]. Therefore, it is highly plausible that isoAsp at residue 55 blocks the cleavage of Asp at residue 57, which resulted in a much longer Asp-N H2 peptide of LCC1. By using the selective Asp-N digestion, we confirmed the previous conclusion, where LCC1 and

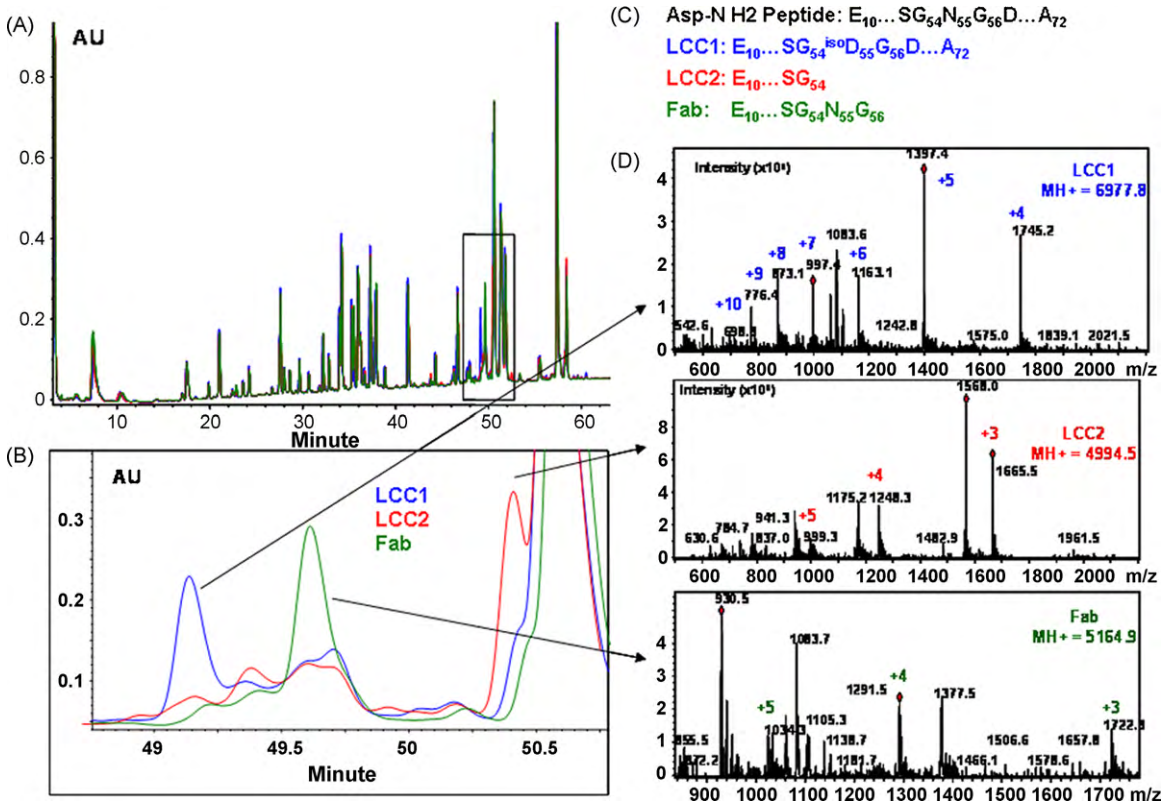

Fig. 8. Comparison of the reduced Asp-N peptide maps of enriched LCC1, LCC2 and Fab. (A) Overlay of the A214 UV traces of LCC1, LCC2 and Fab. (B) Zoomed view between 48 and 51 min elution (boxed area in panel A). (C) Asp-N H2 peptide of LCC1, LCC2 and Fab. (D) Charge state distribution of corresponding peaks.

Table 2
Templates used for homology modeling of mAb1 and mAb2.

Antibody fragment	Template PDB code[a]	Percentage of identity	Template PDB code[a]	Percentage of identity
	mAb1 HC		mAb1 LC	
Framework	1I9R H	79	1I9R L	76
CDR1	3CLF H	100	1EJO L	93
CDR2	3CLF H	88	3DGG A	100
CDR3	1A2Y B	50	1J05 L	88
	mAb2 HC		mAb2 LC	
Framework	3CO8 H	77	3CO8 L	80
CDR1	1MNU H	100	1EFQ A	88
CDR2	2I9L B	76	1EFQ A	100
CDR3	2E27 H	28	1JRH L	63

[a] PDB: Protein Data Bank.

LCC2 have isomerization/deamidation and deamidation at residue 55, respectively.

3.6. Structural analysis

Lys-C/CEX assisted characterization of mAb1 charge variants identified deamidation/isomerization as the reason for the high amount of acidic species in mAb1. Still, the reason for the unique CEX and stability profile of mAb1 was not answered. To investigate the reason for the unique profile, the mAb1 sequence was evaluated and compared to other IgG1 sequences. The sequence alignment identified two IgG1 s (mAb1 and mAb2) containing Asn at position 55 (Kabat numbering). The absence of Asn at the 55 location could explain the simple CEX and stability profile of mAb3 and mAb4 (Figs. 1 and 2). However, mAb1 and mAb2 displayed a completely different CEX profile despite the high sequence similarity, even in the CDR regions.

To understand this, we built an unbiased model of mAb1 and mAb2 (Fig. 9A). The identified templates for the framework regions and CDRs are provided in Table 2. As can be seen in the table, except for the mAb1 HC CDR3, all other peptides shared greater than or equal to 50% sequence identity with the templates. It has been shown that reliable models can be built through a homology modeling procedure provided the percentage of identity with the template is greater than or equal to 30%. The backbone conformation of the loop in which the HC Asn55 is located was similar when mAb1 and mAb2 were compared. Solvent accessibility to water, which is essential for the hydrolysis reaction and structural constraints caused by the protein tertiary structure can affect the deamidation/isomerization rate [37]. Pro53 in mAb2 (Ser53 in mAb1) is likely to restrain the loop since proline in the backbone is constrained due to the ring structure. Gly54 in mAb1 (Arg54 in mAb2) and Gly56 in mAb1 (Asp56 in mAb2) are likely to impart higher flexibility to the loop as glycine lacks a side chain and its backbone can have a larger conformational space compared to the other amino acids with side chains. High propensity of isoAsp formation at Asn-Ser or Asn-Gly was reported previously [38]. For the solvent accessibility, Asn 55 in mAb2 is flanked by two bulky residues, Arg54 and Tyr57. In contrast, Asn55 in mAb1 is flanked by two smaller residues, Gly54 and Asp57. This would make Asn 55 in mAb1 more solvent accessible compared to Asn55 in mAb2. Indeed, solvent accessibility surface area calculations carried out on the models show that Asn55 in mAb1 is 10% more solvent accessible than mAb2. It must be noted here that this difference is likely to increase due to the side chain conformational flexibility in solution.

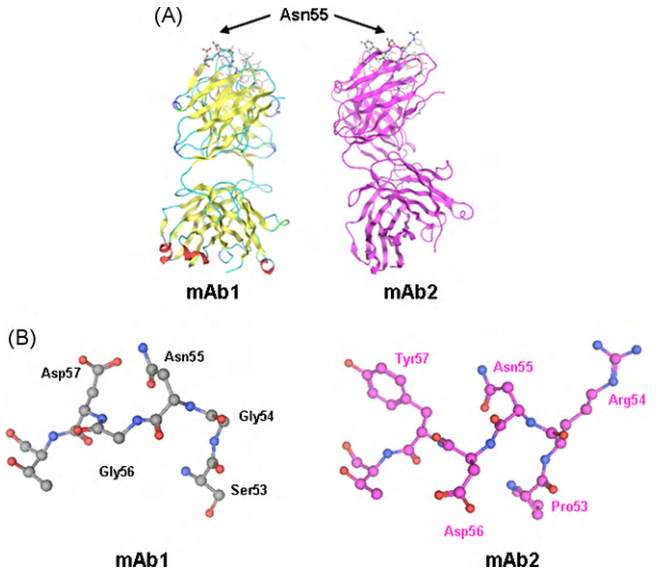

Fig. 9. Model building of mAb1 and mAb2. (A) Ribbon diagram of Fab area of mAb1 and mAb2. (B) Stick diagram of the loop containing Asn55 of mAb1 and mAb2 with the same orientation.

4. Conclusion

The market for mAbs is the fastest growing segment in the pharmaceutical industry. Regulatory expectation has also increased with a high level of scrutiny on impurities and charge heterogeneities. Charge based chromatography has been popular to assess mAb charge heterogeneities. However, the complexity of the profile can be a challenge for the characterization of each variant. Here, we used three combinatorial approaches to understand the unusual CEX profile and instability of a mAb (mAb1). First, by biophysical analysis and peptide mapping, we could pinpoint the Asn55 chemical modification as a reason for the unique mAb1 CEX profile. Second, the limited Lys-C/CEX method was used to separate isoAsp55, which co-eluted with unmodified Asn55 in the peptide map and was indistinguishable by that method. By combining isoAsp55 and Asp55, we could account for almost all of the acidic peak 2 species. This explanation was also applicable to the acidic peak 1 species. Additional chemical modification in the acidic peak 1 could explain the different elution compared to the acidic peak 2 species. Finally, by analyzing the primary sequence and modeling, we could explain the unique mAb1 CEX and stability profile. This combinatorial approach proved very effective in understanding the mAb1 CEX charge variant and stability profile and could be used for characterizing other mAbs.

Acknowledgements

The authors thank Michael Treuheit and David Hambly for a critical review of the manuscript. The authors acknowledge Vladimir Razinkov for technical advice and thank Sihong Deng and Phil Campbell for providing mAb3 and mAb4 stability data.

References

[1] D. Schrama, R.A. Reisfeld, J.C. Becker, Nat. Rev. Drug Discov. 5 (2006) 147.
[2] J.M. Reichert, V.E. Valge-Archer, Nat. Rev. Drug Discov. 6 (2007) 349.
[3] J.L. Cleland, M.F. Powell, S.J. Shire, Crit. Rev. Ther. Drug Carrier Syst. 10 (1993) 307.
[4] M.C. Manning, K. Patel, R.T. Borchardt, Pharm. Res. 6 (1989) 903.
[5] J. Rousseaux, R. Rousseaux-Prevost, H. Bazin, Methods Enzymol. 121 (1986) 663.
[6] J. Rousseaux, R. Rousseaux-Prevost, H. Bazin, J. Immunol. Methods 64 (1983) 141.
[7] J. Rousseaux, G. Biserte, H. Bazin, Mol. Immunol. 17 (1980) 469.
[8] H.S. Gadgil, P.V. Bondarenko, G.D. Pipes, T.M. Dillon, D. Banks, J. Abel, G.R. Kleemann, M.J. Treuheit, Anal. Biochem. 355 (2006) 165.
[9] G.R. Kleemann, J. Beierle, A.C. Nichols, T.M. Dillon, G.D. Pipes, P.V. Bondarenko, Anal. Chem. 80 (2008) 2001.
[10] K. Masuda, Y. Yamaguchi, K. Kato, N. Takahashi, I. Shimada, Y. Arata, FEBS Lett. 473 (2000) 349.
[11] B. Yan, J. Valliere-Douglass, L. Brady, S. Steen, M. Han, D. Pace, S. Elliott, Z. Yates, Y. Han, A. Balland, W. Wang, D. Pettit, J. Chromatogr. A 1164 (2007) 153.
[12] K.G. Moorhouse, W. Nashabeh, J. Deveney, N.S. Bjork, M.G. Mulkerrin, T. Ryskamp, J. Pharm. Biomed. Anal. 16 (1997) 593.
[13] T.M. Dillon, P.V. Bondarenko, D.S. Rehder, G.D. Pipes, G.R. Kleemann, M.S. Ricci, J. Chromatogr. A 1120 (2006) 112.
[14] T.M. Dillon, P.V. Bondarenko, M. Speed Ricci, J. Chromatogr. A 1053 (2004) 299.
[15] L. Huang, J. Lu, V.J. Wroblewski, J.M. Beals, R.M. Riggin, Anal. Chem. 77 (2005) 1432.
[16] M. Adamczyk, J.C. Gebler, J. Wu, J. Immunol. Methods 237 (2000) 95.
[17] H. Lau, D. Pace, B. Yan, T. McGrath, S. Smallwood, K. Patel, J. Park, S.S. Park, R.F. Latypov, J. Chromatogr. B Anal. Technol. Biomed. Life Sci. 878 (2010) 868.
[18] R.J. Harris, B. Kabakoff, F.D. Macchi, F.J. Shen, M. Kwong, J.D. Andya, S.J. Shire, N. Bjork, K. Totpal, A.B. Chen, J. Chromatogr. B Biomed Sci. Appl. 752 (2001) 233.
[19] Y.R. Hsu, W.C. Chang, E.A. Mendiaz, S. Hara, D.T. Chow, M.B. Mann, K.E. Langley, H.S. Lu, Biochemistry 37 (1998) 2251.
[20] K. Patel, R.T. Borchardt, Pharm. Res. 7 (1990) 787.
[21] T. Geiger, S. Clarke, J. Biol. Chem. 262 (1987) 785.
[22] N.E. Robinson, A.B. Robinson, Proc. Natl. Acad. Sci. U.S.A. 98 (2001) 4367.
[23] A.A. Kosky, U.O. Razzaq, M.J. Treuheit, D.N. Brems, Protein Sci. 8 (1999) 2519.
[24] N.E. Robinson, A.B. Robinson, Proc. Natl. Acad. Sci. U.S.A. 98 (2001) 944.
[25] N.E. Robinson, Z.W. Robinson, B.R. Robinson, A.L. Robinson, J.A. Robinson, M.L. Robinson, A.B. Robinson, J. Pept. Res. 63 (2004) 426.
[26] R. Tyler-Cross, V. Schirch, J. Biol. Chem. 266 (1991) 22549.
[27] D. Chelius, D.S. Rehder, P.V. Bondarenko, Anal. Chem. 77 (2005) 6004.
[28] A.A. Shukla, B. Hubbard, T. Tressel, S. Guhan, D. Low, J. Chromatogr. B Anal. Technol. Biomed. Life Sci. 848 (2007) 28.
[29] L.W. Dick Jr., D. Qiu, D. Mahon, M. Adamo, K.C. Cheng, Biotechnol. Bioeng. 100 (2008) 1132.
[30] R.J. Harris, J. Chromatogr. A 705 (1995) 129.
[31] Y. Lyubarskaya, D. Houde, J. Woodard, D. Murphy, R. Mhatre, Anal. Biochem. 348 (2006) 24.
[32] B.A. Johnson, J.M. Shirokawa, W.S. Hancock, M.W. Spellman, L.J. Basa, D.W. Aswad, J. Biol. Chem. 264 (1989) 14262.
[33] Y. Sadakane, T. Yamazaki, K. Nakagomi, T. Akizawa, N. Fujii, T. Tanimura, M. Kaneda, Y. Hatanaka, J. Pharm. Biomed. Anal. 30 (2003) 1825.
[34] R.C. Stephenson, S. Clarke, J. Biol. Chem. 264 (1989) 6164.
[35] W. Zhang, J.M. Czupryn, P.T. Boyle Jr., J. Amari, Pharm. Res. 19 (2002) 1223.
[36] D.M. Hambly, D.D. Banks, J.L. Scavezze, C.C. Siska, H.S. Gadgil, Anal. Chem. 81 (2009) 7454.
[37] S.J. Wearne, T.E. Creighton, Proteins 5 (1989) 8.
[38] D.W. Aswad, M.V. Paranandi, B.T. Schurter, J. Pharm. Biomed. Anal. 21 (2000) 1129.